Research Square

Preprints are preliminary reports that have not undergone peer review.
They should not be considered conclusive, used to inform clinical practice,
or referenced by the media as validated information.

Heterologous Expression, Enzymatic Characterization, and Application of β-Glucuronidase from the Thermophilic Archaeon Dictyoglomus

Mengru Li
Anhui Province Key Laboratory of Pollutant Sensitive Materials and Environmental Remediation, Huaibei Normal University

Qing Guo
Anhui Chem-Bright Bioengineering Co., Ltd

Mingfang Ren
Anhui Province Key Laboratory of Pollutant Sensitive Materials and Environmental Remediation, Huaibei Normal University

Chao Wang
Anhui Province Key Laboratory of Pollutant Sensitive Materials and Environmental Remediation, Huaibei Normal University

Yu Yang
Anhui Province Key Laboratory of Pollutant Sensitive Materials and Environmental Remediation, Huaibei Normal University

Youyu Xie
Anhui Province Key Laboratory of Pollutant Sensitive Materials and Environmental Remediation, Huaibei Normal University

Feng Li
Anhui Province Key Laboratory of Pollutant Sensitive Materials and Environmental Remediation, Huaibei Normal University

Xiaomin Wu
Anhui Province Key Laboratory of Pollutant Sensitive Materials and Environmental Remediation, Huaibei Normal University

Dayong Xu
xudy@chnu.edu.cn

Anhui Province Key Laboratory of Pollutant Sensitive Materials and Environmental Remediation, Huaibei Normal University

Research Article

Keywords: β-glucuronidase, glycyrrhizic acid, molecular dynamics simulation

Posted Date: November 9th, 2026

DOI: https://doi.org/10.21203/rs.3.rs-11419001/v1

License: This work is licensed under a Creative Commons Attribution 4.0 International License.
Read Full License

Additional Declarations: No competing interests reported.

Heterologous Expression, Enzymatic Characterization, and Application of β-Glucuronidase from the Thermophilic Archaeon *Dictyoglomus*

Mengru Li[1,2†], Qing Guo[3,4†] , Mingfang Ren[1,2], Chao Wang[1,2], Yu Yang[1,2], Youyu Xie[1,2], Feng Li[1,2], Xiaomin Wu[1,2*] and Dayong Xu[1,2*]

1 Anhui Province Key Laboratory of Pollutant Sensitive Materials and Environmental Remediation, Huaibei Normal University, Huaibei 235000, China;

2 School of Life Sciences, Huaibei Normal University, Huaibei 235000, China

3 Anhui Chem-Bright Bioengineering Co., Ltd., Huaibei 235000, China; liangsui1980@163.com (Q.G.)

4 Anhui Province Engineering Technology Research Center for Livestock By-Product Medical Intermediate Extraction, Huaibei 235000, China

*** Correspondence:** wuxm@chnu.edu.cn (X.W.); xudy@chnu.edu.cn (D.X.)

[†]These authors contributed equally to this work.

Abstract

Background β-Glucuronidase can catalyze the hydrolysis of glycyrrhizic acid to produce high-value derivatives including glycyrrhetic acid monoglucuronide and glycyrrhetic acid, which possess broad application prospects. Nevertheless, the currently reported enzymes generally exhibit low activity, weak hydrolysis efficiency and poor thermostability, which greatly restrict their industrial applications. This study aimed to screen recombinant β-glucuronidase with high activity and high hydrolysis efficiency, and further explore its enzymatic characteristics, catalytic conversion performance on glycyrrhizic acid, and molecular mechanism. This research provides a theoretical basis for the efficient biological preparation of glycyrrhizic acid derivatives and the molecular modification of enzyme.

Results Four recombinant expression strains of *E. coli* Rosetta (DE3)/pET-28a-GUS were constructed in this study to realize the heterologous expression and enzymatic property characterization of four β-glucuronidases. The results showed that the enzyme from *E. coli* Rosetta (DE3)/pET-28a-DthGUS possessed the highest activity of 123 U/μL, with optimal reaction conditions at pH 5.0 and 85°C. The enzyme tended to be inactivated under pH conditions lower than 4.5. K^+, Zn^{2+}, Cu^{2+} and Ca^{2+} were able to enhance enzyme activity, whereas Fe^{2+} and Fe^{3+} completely inactivated the enzyme. After 8 h of hydrolysis under optimal conditions, the hydrolysis rate of glycyrrhizic acid catalyzed by this enzyme reached 98.7%. Molecular dynamics simulation analysis revealed that Tyr153-mediated π-π stacking and amide-π interaction served as the core forces for DthGUS catalysis toward

pNPG, and Trp351-mediated π-alkyl interaction acted as the key mechanism for its catalytic hydrolysis of glycyrrhizic acid. The total binding free energies of DthGUS with pNPG and glycyrrhizic acid were −73.410 ± 12.935 kJ/mol and −88.144 ± 20.512 kJ/mol, respectively, which confirmed its favorable binding capacity and catalytic hydrolysis ability for both substrates.

Conclusion In conclusion, DthGUS presents prominent advantages of high enzymatic activity, excellent thermostability and efficient glycyrrhizic acid hydrolysis capacity, and can efficiently convert glycyrrhizic acid into target derivatives. This study clarified the core catalytic amino acid residues and molecular mechanism of DthGUS, providing theoretical support and modification targets for the biological preparation of glycyrrhizic acid derivatives and the directed molecular modification of DthGUS.

Keywords: β-glucuronidase; glycyrrhizic acid; molecular dynamics simulation

Introduction

β-Glucuronidase (β-glucuronidase, GUS, EC 3.2.1.31) is a key glycosyl hydrolase [1]. This enzyme cleaves the β-glucuronic acid glycosidic bond at the non-reducing end of sugar substrates, hydrolyzes β-glucuronic acid (GlcA) residues, and releases glucuronic acid and corresponding products [2]. GUS is widely present in bacteria, animals and higher plants, but is rare in fungi, with enzymatic activity detected in only five fungal species [3]. β-Glucuronidase serves as a critical catalyst in biotransformation. Xu [4], Kim [5], and Akao [6] identified β-glucuronidase capable of catalyzing glycyrrhizic acid in fungal and intestinal bacterial systems of animals.β-glucuronidase from *Paenibacillus polymyxa* [7] can be employed for bilirubin transformation.

In general, GUS falls into glycoside hydrolase family 2 (GH2). A small proportion of GUS is distributed in the GH1 and GH79 families [8]. Notably, GH1 and GH79 families belong to the glycoside hydrolase GH-A superfamily. GUS possesses extensive application values. Domestic and international studies have explored its use as a reporter gene [9] and a regulator [10] of human diseases, as well as its applications in drug development guidance, pharmaceutical analysis and detection, glycyrrhizic acid bioconversion, and natural product modification [11]. In recent years, research has focused particularly on the glycosyl modification function of GUS. This function enables GUS to remove sugar moieties from natural compounds (e.g., triterpenes, flavonoids, alkaloids and steroids). On that basis, the solubility, biological activity and bioavailability of substrates can be regulated. Thus, GUS becomes a major research hotspot in relevant fields.

Glycyrrhizic acid (GL) belongs to triterpenoid saponins [12] and is the main water-soluble component of licorice. It binds two glucuronic acid moieties at the C3 position. Removal of these two glucuronic acids yields

glycyrrhetic acid (GA). Glycyrrhetic acid monoglucuronide (GAMG) is the product of glycyrrhizic acid hydrolysis, in which one terminal glucuronic acid group is cleaved. Glycyrrhizic acid exhibits multiple pharmacological activities and favorable sweetening properties. It exerts antibacterial, anti-inflammatory [13], antiviral [14], anti-allergic and anti-ulcer effects [15]. Its sweetness is 50–170 times that of sucrose. Notably, it acts as a high-quality natural sweetener. However, its application has notable limitations. Excessive intake can result in mineralocorticoid-like reactions. Consequently, adverse effects (e.g., hypertension, edema, and abnormal heart function) can be generated. Furthermore, its low bioavailability restricts its applications in various fields. Hydrolysis modification can generate two high-quality derivatives, which effectively remedy these drawbacks [16]. GAMG shares a similar molecular structure with GL. Their pharmacological activities show certain similarities [17]. GAMG has moderate polarity. Its absorption, solubility, pharmacological activity and taste are all superior to those of glycyrrhizic acid [18]. As an important natural product, GAMG also possesses numerous prominent physiological activities such as anti-inflammatory, antiviral, and anti-ulcer effects. It has unique properties compared with glycyrrhizic acid. As a natural functional sweetener, monoglucuronic acid glycyrrhizic acid has extremely high sweetness. The sweetness of glycyrrhizic acid is 0.2 times that of GAMG, and the sweetness of sucrose is 1/1000 of that of GAMG. Glycyrrhetic acid (GA) is the complete hydrolysis product of glycyrrhizic acid and is a lipid-soluble substance. This component has abundant biological activity and extremely high application value. It exerts potent anti-inflammatory, antioxidant and cytoprotective effects [19], and it can be applied in skin care, pigmentation fading, and amelioration of various cutaneous inflammatory disorders [20], but also effectively inhibits fat formation and regulates in vivo metabolic disorders [21]. Meanwhile, glycyrrhetic acid also presents favorable anti-tumor activity, specifically suppressing the proliferation of pancreatic ductal adenocarcinoma cells [22, 23], and holds extremely high research value and broad application prospects in both skin care and biomedical research.

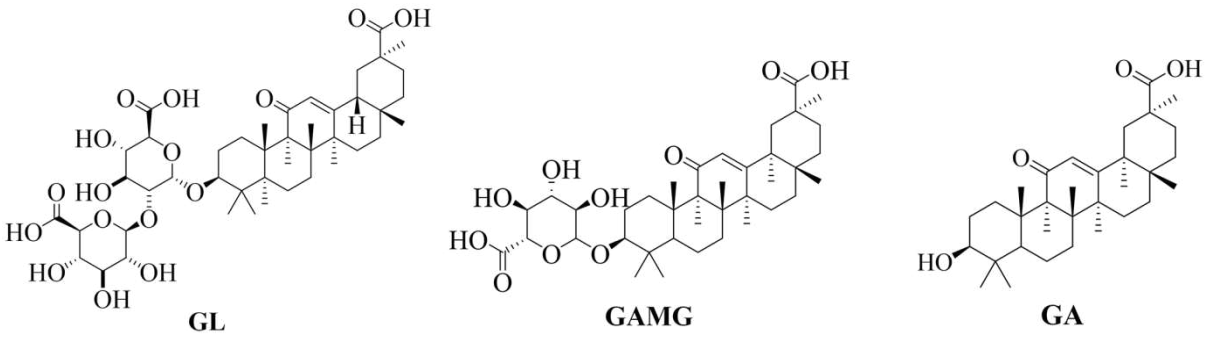


Fig. 1 Chemical structures of glycyrrhizic acid (GL), glycyrrhetinic acid monoglucuronide (GAMG), and glycyrrhetinic acid (GA)

In biotransformation, enzymes serve as core biological catalysts. They have advantages (e.g., greenness, high efficiency, and strong specificity) over traditional chemical catalysis. However, natural enzymes exhibit limited catalytic performance and narrow temperature and pH tolerance ranges. As a result, they are difficult to meet industrial production requirements. Accordingly, enzyme molecular engineering has been used as a key strategy for improving enzymatic activity and promoting the industrialization of biocatalysis [24]. Bioinformatics and enzyme engineering support one another. To be specific, based on computational biology, enzyme structure and function can be analyzed, and active sites and catalytic properties can be predicted. Thus, theoretical foundations can be laid for rational enzyme modification, and development cycles can be shortened [25]. Moreover, experimental data from enzymatic catalysis can be used to refine predictive models continuously. On that basis, the accuracy of intelligent enzyme design and engineering can be enhanced [26].

In this study, four β-glucuronidase target genes were obtained from the genomes of thermophilic archaea. They were heterologously expressed in *E. coli* Rosetta (DE3). Enzymatic and bioinformatics analyses were conducted on the purified β-glucuronidase. For the production of monoglucuronide glycyrrhizin and glycyrrhizin, the enzyme was used to hydrolyze glycyrrhizic acid. This study aims to explore an efficient and environmentally friendly approach for preparing the above-mentioned compounds.

Materials and Methods

Strains and Plasmids

Four codon-optimized β-glucuronidase GUS genes (*DthGUS,* ACI18585.1; *DbGUS*, HOJ92112.1; *DspGUS*, MFN3698646.1; *DtuGUS*, PNV80980.1) were synthesized by Shanghai Sangon Biotech Co., Ltd. The expression plasmid vector adopted was pET-28a(+), and the four distinct recombinant pET-28a(+) plasmids were transformed into competent *E. coli* Rosetta(DE3) cells. The media used in this experiment are listed below:

LB solid medium (g/L): Yeast extract 5, Sodium chloride 10, Peptone 10, Agar 20.

LB liquid medium (g/L): Yeast extract 5, Sodium chloride 10, Peptone 10.

Main Reagents and Instruments

Kanamycin, chloramphenicol, sodium carbonate, imidazole, Tris, SDS, DTT, and pNPG were obtained from Shanghai Sangon Biotech Co., Ltd.; p-nitrophenyl and IPTG were purchased from Aladdin; tryptone, methanol, sodium chloride, and agar were supplied by Sinopharm Chemical Reagent Co., Ltd.; yeast extract was provided

by OXOID; the UV-Vis spectrophotometer was sourced from Yipu Instrument Manufacturing Co., Ltd.; and the high-performance liquid chromatograph was obtained from Huapu Keli Technology Co., Ltd.

Multiple sequence alignment analysis of amino acid sequences of four recombinant β-glucuronidases

The homology among the amino acid sequences of four β-glucuronidases, i.e., DthGUS, DtuGUS, DspGUS, and DbGUS, was analyzed through Multiple Sequence Alignment (MSA). Global alignment was conducted using sequence alignment software. The comparison results were colored according to conservation. To be specific, red areas represent highly conserved amino acid sites. Pink areas represent partially conserved sites. White areas are different sites. Sequence alignment visualization was performed. The amino acid lengths, conserved domains, and amino acid mutation sites of the respective sequence were compared for analyzing sequence differences between DthGUS and other homologous GUS enzymes and identifying key amino acid residues [27].

Expression and Purification of Four Recombinant β-Glucuronidase Proteins

Four different GUS gene coding sequences were used as target fragments to construct four recombinant expression vectors based on the pET28a(+) system. The target fragments with specific primers were amplified, and corresponding restriction enzyme sites were introduced. Next, the fragments were digested with two restriction enzymes along with linearized pET28a(+) vector. Following this step, gel purification was carried out. Using T4 DNA ligase, we ligated the purified fragments to the vector. The ligation products were transformed into competent DH5α cells. On LB plates containing kanamycin and chloramphenicol, colonies were selected. For colony PCR screening, single colonies were selected. Plasmid DNA from positive clones was extracted. For electrophoretic verification, the extracted clones were subjected to double digestion with restriction enzymes. Recombinant plasmids were validated through restriction analysis. They were subjected to sequencing to confirm that all four inserted GUS sequences were mutation-free and maintained intact reading frames. Subsequently, the four correctly sequenced recombinant plasmids were transformed into *E. coli* Rosetta(DE3) competent cells and plated on LB agar containing kanamycin and chloramphenicol. Four engineered expression strains, i.e., Rosetta(DE3)/pET28a-DthGUS, Rosetta(DE3)/pET28a-DbGUS, Rosetta(DE3)/pET28a-DspGUS, and Rosetta(DE3)/pET28a-DtuGUS, were obtained. The recombinant strains were activated on kanamycin- and chloramphenicol-supplemented LB plates and incubated overnight at 37°*C.* After colony formation, single colonies were picked and inoculated into 5 mL of liquid LB medium containing the two antibiotics for overnight cultivation. The cultures were then transferred at a 1% inoculum to 500 mL of liquid LB medium containing kanamycin and chloramphenicol and grown at 37°C and 220 rpm until the optical density reached 0.6–0.8. IPTG

was added to the cultures at a final concentration of 0.5 mM, and protein expression was induced at 16°C and 220 rpm for 16–18 h. Upon induction completion, the cultures were centrifuged at 8,000 rpm for 10 min; the supernatants were discarded, and the cell pellets were harvested and stored at -80°C for subsequent experiments.

The four cell precipitates were resuspended in lysis buffer [20 mM Tris-HCl (pH 8.0), 500 mM NaCl, 5 mM imidazole] at a ratio of 1 g: 10 mL. The mixtures were thoroughly vortexed until no visible clumps remained. Next, disruption was carried out using an ultrasonic homogenizer. The lysates were centrifuged at 8,000 rpm for 10 min at 4°C. The supernatants were collected as crude enzyme solutions. The four recombinant β-glucuronidases were purified through Ni-NTA affinity chromatography. The nickel column was equilibrated with five column volumes of equilibration buffer [20 mM Tris-HCl (pH 8.0), 500 mM NaCl, 5 mM imidazole]. The crude enzyme solution was filtered through a 0.22 μm membrane. The filtered crude enzyme was loaded onto the purification column. After sample loading, the column was washed with five column volumes of wash buffer [20 mM Tris-HCl (pH 8.0), 500 mM NaCl, 100 mM imidazole] to remove non-specifically bound impurities. Target proteins were eluted sequentially using five column volumes of elution buffers with gradient imidazole concentrations [20 mM Tris-HCl (pH 8.0), 500 mM NaCl, 150 mM imidazole; 200 mM imidazole; 500 mM imidazole], with each elution fraction collected separately. All collected fractions were transferred into dialysis bags and dialyzed against dialysis buffer 1 [20 mM Tris-HCl (pH 8.0), 500 mM NaCl, 1 mM DTT] with continuous stirring overnight using a magnetic stirrer. The next day, the buffer was replaced with dialysis buffer 2 [20 mM Tris-HCl (pH 8.0), 150 mM NaCl, 1 mM DTT], and dialysis was continued for another 6–8 h to obtain purified enzymes [28]. SDS-PAGE analysis was performed to identify the optimal imidazole concentration for target protein elution. All the aforementioned buffers consist of Tris-HCl, NaCl and imidazole, with differences only in solute concentrations. Tris stabilizes pH, NaCl reduces electrostatic non-specific binding, and imidazole competes for nickel binding sites. On that basis, immobilization, impurity removal and gradient elution can be achieved.

Fermentation Optimization and Enzymatic Properties of Four Recombinant β-Glucuronidases

Optimization of Fermentation Process Parameters

In this study, the fermentation and induction parameters in *E. coli* were optimized to enhance the solubility and enzymatic activity of recombinant GUS protein. First, the effect exerted by IPTG induction concentration on bacterial growth and GUS expression was investigated. IPTG induced the expression of the target gene in the host strain. The IPTG concentration was optimized and combined with low temperature and appropriate induction duration. On that basis, the proper folding of the recombinant protein was promoted, incorrect aggregation was

reduced, and the proportion of soluble active protein was elevated. Accordingly, optimal conditions for GUS enzyme activity expression were achieved.

In this experiment, ten IPTG concentration gradients were established, i.e., 0.1 mM, 0.2 mM, 0.3 mM, 0.4 mM, 0.5 mM, 0.6 mM, 0.7 mM, 0.8 mM, 0.9 mM, and 1.0 mM, to investigate their effects on bacterial growth and GUS enzyme production. Bacterial cultures were grown at 37 °C with shaking at 220 rpm until the OD_{600} reached 0.6–0.8. Subsequently, different concentrations of IPTG were added. Induction was carried out at 16°C and 220 rpm for 16–18 h. Three biological replicates were covered in the respective group.

Induction temperature serves as a critical factor affecting the soluble expression of foreign proteins in Escherichia coli. High temperatures accelerate protein synthesis but may result in insufficient folding of newly synthesized proteins. Consequently, aggregation into inclusion bodies can be triggered, and the yield of soluble, active protein can be reduced. Moderately lowering the induction temperature slows down protein synthesis, which can provide sufficient time for proper protein folding, reduce inclusion body formation, and upregulate the soluble expression level of GUS. Based on the optimal IPTG concentration, the effects of induction temperature on bacterial growth and GUS expression were investigated using five temperature gradients, i.e., 16 °C, 20 °C, 25 °C, 30 °C, and 37 °C. Bacterial cultures were initially grown at 37°C and 220 rpm until reaching an OD_{600} of 0.6–0.8. IPTG was then added, and the cultures were transferred to respective pre-set induction temperatures for constant-temperature induction at 220 rpm for 16–18 h.

Optimal Conditions and Stability Determination

β-glucuronidase is capable of hydrolyzing the substrate 4-nitrophenyl-β-D-glucuronide (pNPG) for the production of p-nitrophenol. We determined the enzymatic activity of β-glucuronidase by hydrolyzing substrate pNPG using a standard curve of varying concentrations of p-nitrophenol dissolved in 50 mM acetic acid-acetate sodium buffer. p-nitrophenol was quantitatively detected at 405 nm with a spectrophotometer. The enzyme activity was calculated [29].

With the same cell concentration and pNPG as substrate, the optimal reaction pH of GUS was determined at 85 °C. 10 μL of the enzyme solution was accurately transferred and added to 40 μL of buffer containing 1.25 mM pNPG at different pH values (pH 4.0, 4.5, 5.0, 5.5, 6.0; 50 mM acetic acid-acetic acid sodium buffer and pH 6.5, 7.0, 7.5, 8.0; 50 mM Tris-HCl buffer) at 85 °C. After 10 min of reaction, 200 μL of 0.4 M Na2CO3 solution was added to stop the reaction. For pH stability measurement, the above method was used. A certain volume of enzyme solution was accurately taken and added to different pH buffers for even mixing. The sample was incubated at 4 °C for 30 min. The residual activity of the enzyme solution was tested.

A temperature gradient was set as 30 °C, 35 °C, 40 °C, 45 °C, 50 °C, 55 °C, 60 °C, 65 °C, 70 °C, 75 °C, 80 °C, 85 °C, and 90 °C for determining the optimal reaction temperature of GUS. Ten microliters of enzyme solution were added to 40 μL of optimal pH buffer and incubated at the respective temperature for 10 min. We mixed a certain amount of enzyme solution thoroughly with optimal pH buffer for assessing thermal stability. The mixture was incubated at different temperatures for 30 min. After the incubation, the mixture was cooled on ice. Next, the residual enzyme activity was measured.

Prepare ionic solutions of required concentrations, mix enzyme solution with each ionic solution evenly so that the final concentration of each ion reaches 2 mM. Incubate at 4 °C for 30 min. Detect residual enzyme activity under optimal pH and temperature. All experiments used inactivated enzyme solution as the control group (CK), and three parallel tests were set up [30].

To screen the enzyme with the best catalytic activity, we compared and evaluated the enzymatic activities of four recombinant β-glucuronidases, examined the catalytic performance of different enzymes, and selected the β-glucuronidase with the highest enzymatic activity.

Conversion of glycyrrhizic acid into glycyrrhetinic acid monoglucuronide and glycyrrhetinic acid by four recombinant β-glucuronidases

Dissolve glycyrrhizic acid in pH 5.0, 50 mM acetic acid - sodium acetate buffer, and prepare the substrate solution (with a glycyrrhizic acid concentration of 10 mg/mL). According to the volume ratio of enzyme solution to substrate liquid of 1:4, add the four recombinant β-glucuronidase solutions respectively to the glycyrrhizic acid substrate solution, and carry out the biotransformation reaction under an oscillating condition at 85 ℃. Take samples at 8 hours, add methanol to terminate the enzymatic reaction. The samples are centrifuged (12,000 × g, 10 min), and the supernatant is passed through a 0.22 μm organic filter membrane. Use HPLC to simultaneously detect GL, GAMG and GA, and calculate the glycyrrhizic acid hydrolysis conversion rate based on the HPLC quantitative data. A C_{18} reversed-phase chromatography column (250 mm × 4.6 mm, 5 μm) was applied, with detection wavelength of 254 nm, flow rate of 1.0 mL/min, column temperature of 30 °C, and injection volume of 10 μL; methanol served as mobile phase B and 0.5% aqueous acetic acid as mobile phase A for gradient elution: 0–15 min, keep 75% phase B; 15–16 min, 75%–85% phase B; 16–31 min, keep 85% phase B; 31–32 min, 85%–95% phase B; 32–40 min, keep 95% phase B.

Enzyme Kinetic Parameter Determination

Based on the above results, the recombinant β-glucuronidase with the highest enzyme activity and hydrolysis rate was selected. Prepare pNPG solutions at concentrations of 1 mM, 2 mM, 3 mM, 4 mM, 5 mM, and 6 mM using 50

mM acetate-sodium acetate buffer (pH 5.0) as the substrate. Add 10 μL of enzyme solution to 40 μL of buffer, incubate for 10 min at the optimal reaction temperature, then measure the concentration of p-nitrophenol. The Lineweaver-Burk plot method was used to calculate the enzyme kinetic parameters.

Catalytic Mechanism of Recombinant β-Glucuronidase in Hydrolyzing pNPG and Glycyrrhizic Acid

Based on the above results, the recombinant β-glucuronidase with the highest enzyme activity and hydrolysis rate was selected. Since no resolved protein crystal structure of GUS is available in the PDB database, we adopted the GUS structure predicted by AlphaFold2 software [31]. The GUS amino acid sequence was processed using python3 to execute the run_docker.py script, and the three-dimensional structure model of GUS built by AlphaFold2 was obtained. pNPG and glycyrrhizic acid were separately docked with the GUS protein system via the online SWISSDOCK docking platform (https://www.swissdock.ch/). The best binding conformation was chosen for molecular dynamics simulation to reach a stable equilibrium state. The binding stability, kinetic characteristics, and thermodynamic properties derived from simulation trajectories were analyzed to clarify the intrinsic mechanism underlying its catalysis toward pNPG and glycyrrhizic acid.

Results

Multiple sequence alignment analysis of amino acid sequences of four recombinant β-glucuronidases

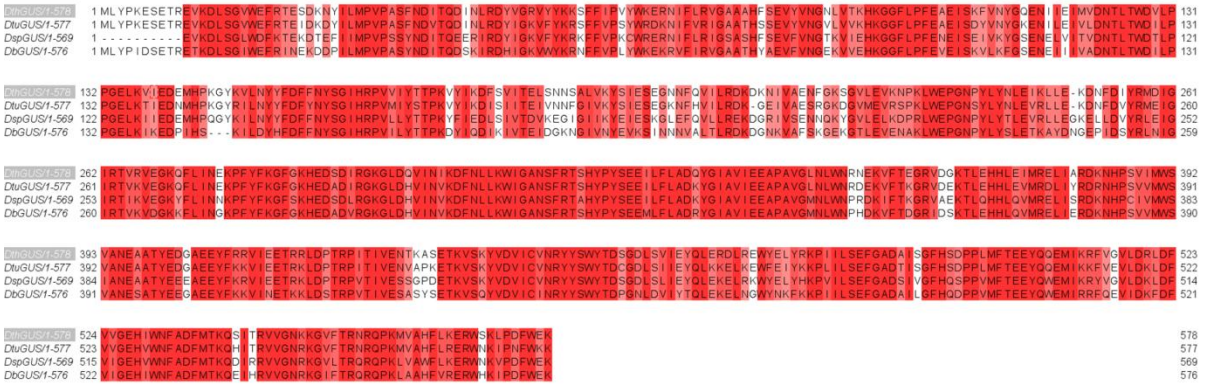


Fig. 2 Comparison of amino acid sequence conservation and differential sites of four β-glucuronidase enzymes

The multiple sequence alignment results are presented in the figure. The overall amino acid sequence homology among the four β-glucuronidases is relatively high, and numerous amino acid positions are highly conserved (red regions are distributed across the whole peptide chain), suggesting that the core domain and catalytic-related sites of this enzyme family are highly conserved. Meanwhile, multiple amino acid residue

variation sites exist between these sequences. Such differences may constitute the molecular basis for variations in enzymatic properties including catalytic activity and substrate selectivity (hydrolysis of glycyrrhizic acid to produce GAMG and GA) among different β-glucuronidases. Amino acid conservation slightly decreases in the terminal regions of the sequences, and minor differences are observed in sequence length. The full length of DthGUS is 578 aa, DbGUS is 576 aa, DspGUS is 569 aa, and DtuGUS is 577 aa.

Construction and Expression of Recombinant Plasmid

SDS-PAGE results indicated that all four recombinant proteins were successfully expressed in *E. coli* Rosetta (DE3), and the target proteins were detected in both the soluble supernatant and pellet fractions. However, target protein of DspGUS could not be recovered under this purification condition, whereas the other three recombinant proteins could be eluted using 150 mM imidazole to obtain target products. By comparison with protein molecular weight markers, the molecular weights of these three recombinant β-glucuronidases were approximately 60 kDa.

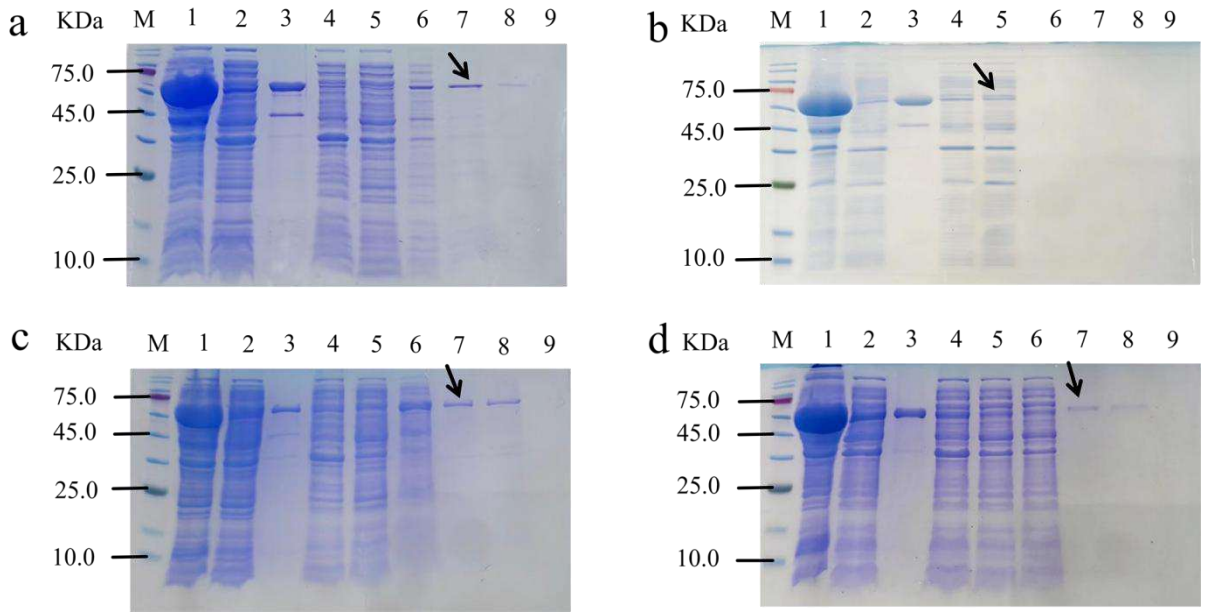


Fig. 3 SDS-PAGE analysis of four recombinant β-glucuronidase variants. **(a)** DthGUS; **(b)** DspGUS; **(c)** DbGUS; **(d)** DtuGUS. In each figure, M represents the protein Marker, and Channels 1–9 have the same treatment conditions. M: protein Marker; Channel 1: total protein after lysis; Channel 2: supernatant after lysis; Channel 3: precipitate after lysis; Channel 4: flow through fluid; Channel 5: 50 mM imidazole elution; Channel 6: 100 mM imidazole elution; Channel 7: 150 mM imidazole elution; Channel 8: 200 mM imidazole elution; Channel 9: 500 mM imidazole elution; Arrow: target protein

Fermentation Optimization and Enzymatic Properties of Four Recombinant β-Glucuronidases

Optimization of Fermentation Process Parameters

Fig. 4(a) shows that different IPTG concentrations exert a notable effect on the soluble expression of β-glucuronidase. When the inducer concentration ranges from 0.1 mM to 1.0 mM, the enzyme activity shows an upward trend as the induction concentration increases. When the IPTG concentration reaches 0.5 mM, the enzyme activity reaches the highest. However, if the inducer concentration increases further, the enzyme activity value displays a downward trend. The experimental result shown in Fig. 4(b) reveals that among the five tested temperature gradients, enzyme activity peaks at 16 °C and reaches the lowest value at 37 °C. Enzyme activity of β-glucuronidase gradually decreases as temperature rises; thus, 16 °C was selected as the induction temperature.

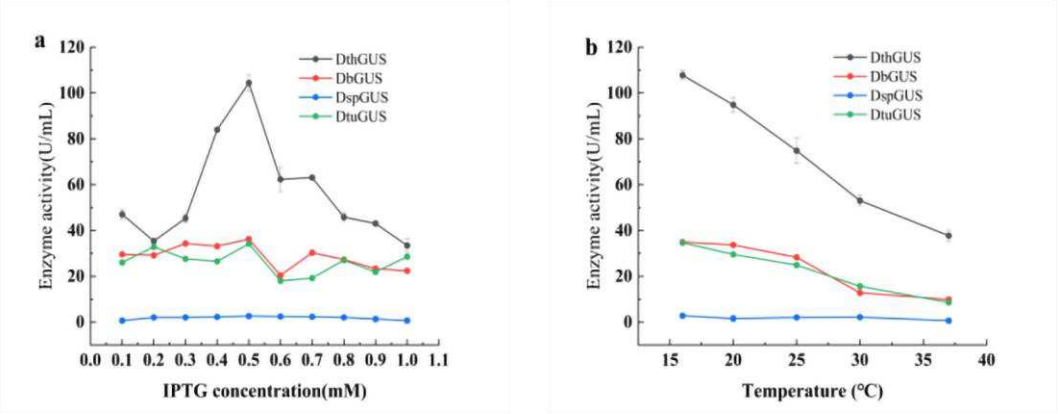


Fig. 4 Parameter optimization of the fermentation process for four recombinant β-glucuronidases. **(a)** effect of inducer concentration on enzyme activity; **(b)** effect of induction temperature on enzyme activity

Optimal Conditions and Stability Determination

Temperature serves as a vital factor affectingβ-glucuronidase's activity and structural stability. As depicted in Fig. 5(a), the optimal reaction temperature for DthGUS is 85 °C. At this temperature, the enzyme activity reaches its peak. As indicated by the thermal stability results (Fig. 5(b)), this enzyme exhibits high thermal stability in the range of 30–95 °C. It can maintain high catalytic activity over extended periods. However, when the temperature rises to 100 °C, enzyme activity significantly declines, nearly losing all catalytic function. DbGUS, DspGUS, as well as DtuGUS have an optimal reaction temperature of 75 °C. At this optimal temperature, their activities can reach maximum levels. As indicated by thermal stability tests, the above-mentioned three enzymes remain stable between 30–75 °C, sustaining high enzymatic activity for prolonged durations. When temperatures increase to the range of 80–100 °C, their activities decrease significantly until complete inactivation occurs.

Significant differences can be found in the optimal pH and pH stability of GUS enzymes from different sources. Enzymes exhibit their optimal catalytic performance at their optimal pH values. However, fluctuations in environmental pH can alter the enzyme protein's spatial conformation. Thus, the activity, structural stability, and catalytic function of the protein can be significantly affected. As depicted in Fig. 5(c), DthGUS achieves an optimal pH of 5.0, and its maximum enzyme activity reaches 98.4 U/μL. Enzyme activity tends to increase with rising pH in the range of 4.0–5.0 and displays an overall declining trend between pH 5.5 and 8.0. As presented in Fig. 5(d), this enzyme maintains stable activity over a long period within the pH range of 4.0–8.0. DbGUS, DspGUS, and DtuGUS all have an optimal pH of 5.5, with peak activities of 27.6 U/μL, 4.1 U/μL, and 31 U/μL, respectively. The activity profiles of these three enzymes are similar: activity increases progressively in the pH range of 4.0–5.0 and then steadily declines from pH 5.5 to 8.0. To be specific, DbGUS exhibits relatively low activity under strongly acidic conditions but retains high activity for extended periods in the pH range of 5.0–8.0. DtuGUS demonstrates good pH stability across the pH range of 4.0–8.0, maintaining relatively consistent enzyme activity.

The catalytic activity of enzymes can be influenced by metal ions, which may either inhibit or enhance activity. Taking DthGUS as an example, according to the results shown in Fig. 5(e), compared with the control group, Fe^{2+} and Fe^{3+} significantly inhibit ACI185,while Mn^{2+} and Mg^{2+} have no significant effect on enzyme activity. Zn^{2+}, Ga^{2+}, Cu^{2+},Na^{+}, and K^{+} promote ACI185. For the other three GUS enzymes, metal ions exerted no notable activating effect and even inhibited enzyme activity.

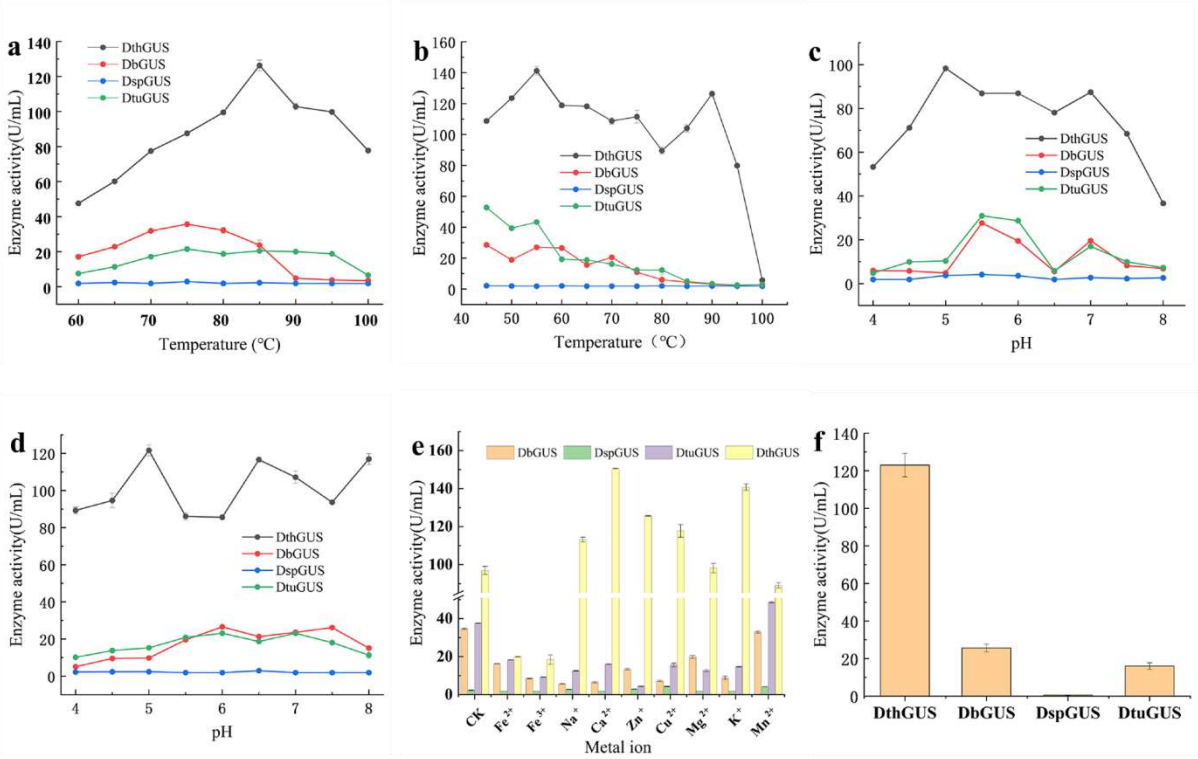


Fig. 5 Enzymatic properties of four recombinant β-glucuronidase variants. **(a)** optimal reaction temperature of GUS; **(b)** temperature stability of GUS; **(c)** optimal reaction pH of GUS; **(d)** pH stability of GUS; **(e)** effects of metal ions on GUS activity; **(f)** comparison chart of enzymatic activity of four recombinant β-Glucuronidase enzymes

Based on the aforementioned results, the enzymatic activities of the four recombinant enzymes were determined under the optimal temperature and pH conditions. The enzymatic activities of the four recombinant enzymes were significantly different (Fig. 5(f)). To be specific, DthGUS exhibited the highest enzymatic activity, approximately 123 U/μL. DbGUS and DtuGUS were second, approximately 26 U/μL and 16 U/μL respectively. DspGUS showed almost no enzymatic activity. This result also corroborates the protein purification results. In conclusion, DthGUS exhibited the optimal catalytic activity and can be considered a more ideal candidate enzyme for subsequent catalytic application research.

Four recombinant β-glucuronidases for the conversion of glycyrrhizic acid into monoglucuronide glycyrrhizin and glycyrrhizin

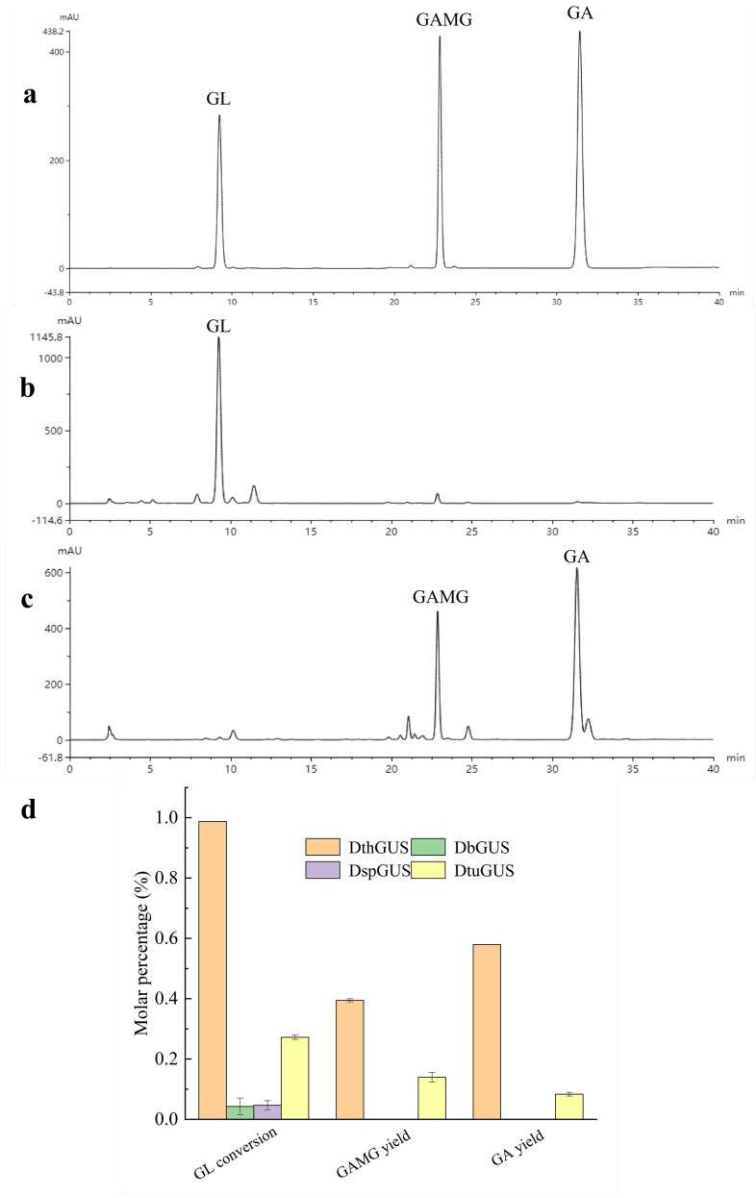


Fig. 6 Analysis of the hydrolysis of glycyrrhizic acid catalyzed by four recombinant β-glucuronidase enzymes. **(a)** HPLC chromatogram of mixed reference standards; **(b)** HPLC diagram of the reaction at 0 h using DthGUS as an example; **(c)** HPLC diagram of the reaction at 8 h using DthGUS as an example; **(d)** hydrolysis rate, yield of GAMG, and yield of GA catalyzed by the four recombinant β-glucuronidase enzymes

As shown in Fig. 6, DthGUS exhibits the maximal catalytic rate for the hydrolysis of glycyrrhizic acid (98.7%). Compared with the traditional hydrolysis process, the glycyrrhizic acid hydrolysis rate of the traditional chemical acidolysis method reaches merely about 80.24%. Besides, it requires high temperature, strong acid, as

well as a long reaction time, which is prone to excessive hydrolysis and difficult to achieve targeted enrichment of GAMG. Although a part of microbial fermentation methods have been found to achieve a relatively high GAMG conversion level, they generally have disadvantages such as long fermentation cycle, complex process, and difficult control of by-products. In this study, DthGUS can achieve a high substrate hydrolysis rate of 98.7% under mild reaction conditions, which is significantly superior to the traditional acidolysis process. The yield of the target product GAMG can reach 39.5%, and the yield of glycyrrhetic acid is 58%. GAMG can efficiently convert the substrate and obtain two types of hydrolysis products step by step, avoiding the drawback of harsh reaction conditions of the chemical method. It shows good application potential in the rapid and mild preparation of GAMG and glycyrrhetic acid.

As revealed by the above enzymatic property characterization and the results of glycyrrhizic acid hydrolysis effect, the DthGUS protein expressed by the *E. coli* Rosetta (DE3)/pET-28a-DthGUS recombinant strain has excellent catalytic properties. Under experimental conditions, it can achieve high conversion efficiency for glycyrrhizic acid substrate hydrolysis. Compared with the other recombinant β-glucuronidases, this enzyme has obvious advantages in catalytic activity and stability, and has the best overall catalytic performance. Therefore, in this study, DthGUS was selected as the research object, and subsequent bioinformatics analysis was carried out. Based on molecular docking and molecular dynamics simulation methods, we further explained the molecular mechanism underlying its efficient catalysis of glycyrrhizic acid hydrolysis.

Enzyme Kinetics Assay

The DthGUS kinetic parameters were calculated using the double reciprocal plot method, and the results are as follows:

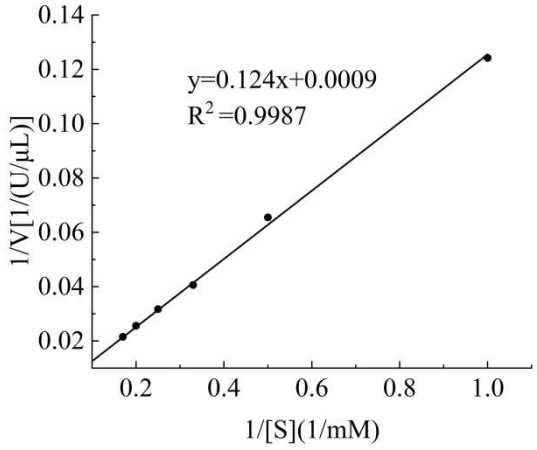


Fig. 7 Enzyme kinetics of DthGUS

Table 1 Enzyme kinetic parameters of DthGUS

Concentration/mM	OD_{405}	Enzyme Activity(U/μL)	1/[S]	1/V
0.4	0.643	82.25	2.5	0.0121
0.6	0.871	110.75	1.667	0.0090
0.8	0.994	126.125	1.25	0.0079
1	1.079	136.75	1	0.007
1.2	1.194	151.125	0.833	0.0066
1.4	1.318	166.625	0.714	0.0060

As shown in Fig. 7, the kinetic parameters of *E. coli* Rosetta(DE3)/pET-28a-DthGUS are:V_{max} = 263 U/μL, Km = 0.87 mM.

Catalytic Mechanism of Recombinant β-Glucuronidase in Hydrolyzing pNPG and Glycyrrhizic Acid

Recombinant β-glucuronidase hydrolyzes pNPG

In this study, the static binding mode of DthGUS with the substrate pNPG through molecular docking was analyzed (Fig. 8a, 8b). As indicated by the results, pNPG could precisely fit into the active cavity of DthGUS. The above binding pocket was composed of key residues (e.g., Tyr152, Tyr153, Phe154, Asp155, His321, Trp351, Asn395, Glu396, and Arg543). This result demonstrates that DthGUS has a tight and high-affinity binding with pNPG and possesses a good substrate binding foundation.

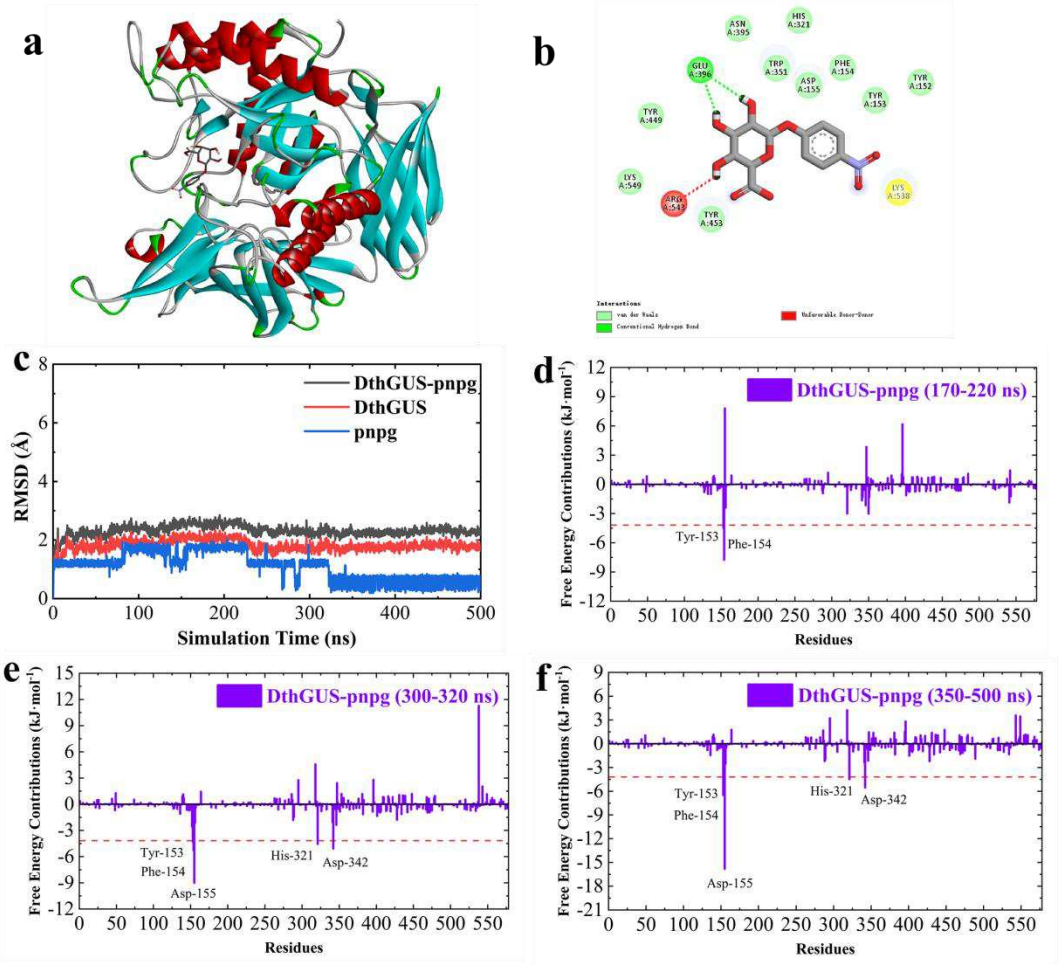


Fig. 8 Binding mode of DthGUS with pNPG and molecular dynamics simulation results of the DthGUS-pNPG complex**. (a)** the docking binding mode of DthGUS and pNPG; **(b)** the structure of pNPG; **(c)** the RMSD (root mean square deviation) change curves of the DthGUS monomer, the pNPG ligand, and the DthGUS-pNPG complex during the 500 ns molecular dynamics simulation process; **(d-f)** the contribution of each amino acid residue to the binding free energy of the DthGUS-pNPG complex in the simulation time periods of 170–220 ns, 300–320 ns, and 350–500 ns. The red dotted lines mark the key residues with significant contributions

However, molecular docking can merely present static binding characteristics and cannot indicate the dynamic conformational stability and kinetic change patterns of the complex in the solution system. Therefore, the optimal conformation of the molecular docking complex was screened in this study. Moreover, to systematically explore the dynamic binding characteristics and conformational evolution features of the DthGUS-pNPG complex, a 500 ns molecular dynamics (MD) simulation was performed based on the RSFF2C force field.

As depicted in Fig. 8(c), the DthGUS-pNPG complex and DthGUS show a slight increase at the initial stage and then maintain a stable trend. From 0 to 30 ns, it is a slight increase. From 30 to 220 ns, it remains stable,

stabilizing at 2.4 Å and 2.1 Å, respectively. During the period of 220-240 ns, it slightly decreases. From 240 to 500 ns, it remains in a stable state, respectively stabilizing at 2.2 Å and 1.9 Å. This indicates that the complex is in a balanced state after 30 ns. The ligand pNPG in the complex system underwent multiple fluctuations, stabilizing at approximately 0.7 Å from 323 to 500 ns. This result indicates that after 323 ns, the complex system is in a highly stable conformational state, which can be used as the conformational basis for subsequent analysis of binding free energy calculation and thermodynamic feature analysis.

The stable equilibrium process of the DthGUS and pNPG complex can be analyzed to acquire information (e.g., the thermodynamic properties of the enzyme catalytic mechanism). The MM/PBSA method was employed for calculating the binding free energy (ΔG_{bind}) value of the GUS-pNPG complex system based on the equilibrium trajectory of the MD simulation in the time period of 170-500 ns. Table 2 lists the energy contribution values of the four components, i.e., van der Waals energy (ΔG_{vdw}), coulombic electrostatic interaction energy (ΔG_{ele}), and polar and non-polar solvation free energy (ΔG_{PB} and ΔG_{SA}). As indicated by the table, the ΔG_{bind} value of the DthGUS-pNPG complex system at 300-500 ns is -73.410 ± 12.935 kJ/mol, which has the most stable range. The calculated ΔG_{vdw} value and ΔG_{ele} value are as high as -124.006 ± 13.26 kJ/mol and -160.789 ± 13.529 kJ/mol respectively, while the ΔG_{SA} free energy value is quite low, with a value of -13.976 ± 0.557 kJ/mol. The calculated ΔG_{PB} free energy value of the complex is 225.361 ± 13.752 kJ/mol. The above-mentioned findings reveal that van der Waals interaction, Coulombic electrostatic interaction, and non-polar solvation interaction are of great significance in the GUS catalyzing the pNPG molecule process, while the strong polar solvation interaction energy exerts an adverse effect on the catalytic process of the DthGUS-pNPG complex. As indicated by these results, there is a strong and stable binding interaction force between DthGUS and pNPG molecules, promoting the recognition and binding of GUS and pNPG molecules and their hydrolytic catalytic action.

In order to further explore which residues in the DthGUS molecule recognition and catalysis process play a significant role in catalyzing the pNPG molecule, we conducted a residue-specific free energy decomposition calculation on the binding free energy of the aforementioned complex. The results are shown in Fig. 8(d-f).

Table 2 Simulated binding free energy of the DthGUS-pNPG complex (unit: kJ/mol)

System	Time scope (ns)	ΔG_{vdw}	ΔG_{ele}	ΔG_{PB}	ΔG_{SA}	ΔG_{bind}
DthGUS-pNPG	170-220	-172.913 ± 11.697	-112.534 ± 16.259	242.404 ± 15.340	-17.078 ± 0.760	-60.121 ± 9.730

300-32	-145.974 ±	-143.984 ±	240.187 ±	-15.074 ±	-64.845 ±
0	10.813	32.907	25.073	0.673	10.511
350-50	-124.006 ±	-160.789 ±	225.361 ±	-13.976 ±	-73.410 ±
0	13.626	13.529	13.752	0.557	12.935

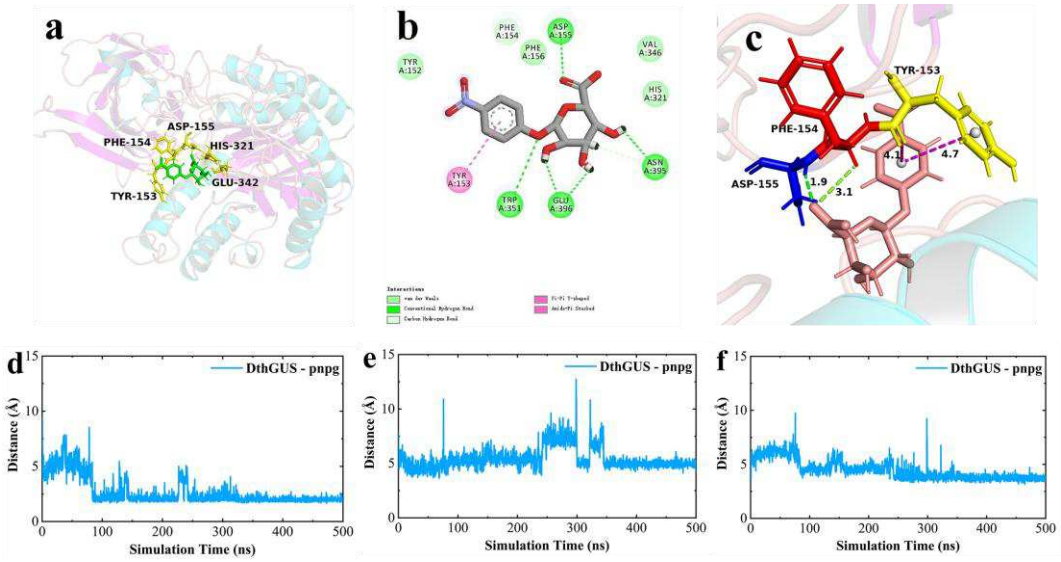


Fig. 9 Analysis of Key Interactions in Molecular Dynamics Simulation of the DthGUS-pNPG System. **(a)** key interactions representing the conformational active site of the DthGUS-pNPG system at equilibrium; **(b)** interaction pattern diagram of the conformation represented by the MD simulation of the DthGUS-pNPG system under the RSFF2C force field. The key residues of DthGUS and the structure of the pNPG molecule are all represented by stick models; **(c)** distance visualization graph of the interaction between the key residues and the pNPG molecule (unit: Å); **(d)** distance variation of the hydrogen bond formed between the key residue Asp155 and the pNPG molecule over time; **(e)** distance variation of the π-π stacking interaction formed between the key residue Tyr153 and the pNPG molecule over time; **(f)** distance variation of the amide stacking interaction formed between the key residue Tyr153 and the pNPG molecule over time

The residue energy decomposition analysis further screened out the core functional residues of the catalytic process (Table 3). In the stable 350-500 ns system interval, the energy contributions of Asp155, Tyr153, and Phe154 were reported as the most significant. To be specific, Asp155 contributed the most. The binding free energy of Tyr153 and Phe154 was -6.498 kJ/mol and -5.743 kJ/mol respectively, which were the key residues maintaining the stable conformation of the complex and ensuring the catalytic activity of DthGUS. The interaction analysis of the active site (Fig. 9) showed that pNPG was stably localized in the active cavity formed

by both polar and non-polar residues. The key residues are capable of forming multiple specific intermolecular interactions: Tyr153 has dual functions; its aromatic ring forms π-π stacking with pNPG, and the amide group can form amide-π interaction with the substrate; Asp155 forms a stable hydrogen bond with pNPG through the amide hydrogen of the peptide bond. Multiple weak interactions cooperate to maintain the complex structure and enable DthGUS to precisely recognize pNPG and efficiently catalyze hydrolysis.

Table 3 Hot spot residue energy decomposition of DthGUS-pNPG(unit: kJ/mol)

System	Time scope (ns)	Residues	ΔG_{MM}	ΔG_{PB}	ΔG_{SA}	ΔG_{bind}
DthGUS-pNPG	170-220	Tyr153	-12.186	8.888	-1.169	-4.480
		Phe154	-11.388	4.011	-0.396	-7.774
	300-320	Tyr153	-12.156	8.500	-0.683	-4.344
		Phe154	-13.556	8.769	-0.510	-5.284
		Asp155	-8.007	-0.232	-0.774	-9.020
		His321	-8.394	4.359	-0.553	-4.577
		Glu342	-7.308	2.226	0	-5.095
	350-500	Tyr153	-13.424	7.645	-0.721	-6.498
		Phe154	-15.002	9.865	-0.611	-5.743
		Asp155	-7.653	-7.382	-0.807	-15.835
		His321	-7.527	3.535	-0.501	-4.494
		Glu342	-7.715	2.169	0	-5.546

Recombinant β-glucuronidase hydrolyzes glycyrrhizic acid

Molecular docking was employed to clarify the static binding mode of DthGUS and glycyrrhizic acid in the preliminary stage of this study. It was confirmed that glycyrrhizic acid could precisely fit into the active cavity of DthGUS. This binding pocket is composed of multiple key amino acid residues (e.g., Arg543, Tyr449, His321, Asp155, and Trp351), which can lay a structural basis for the specific binding of the enzyme and the substrate.

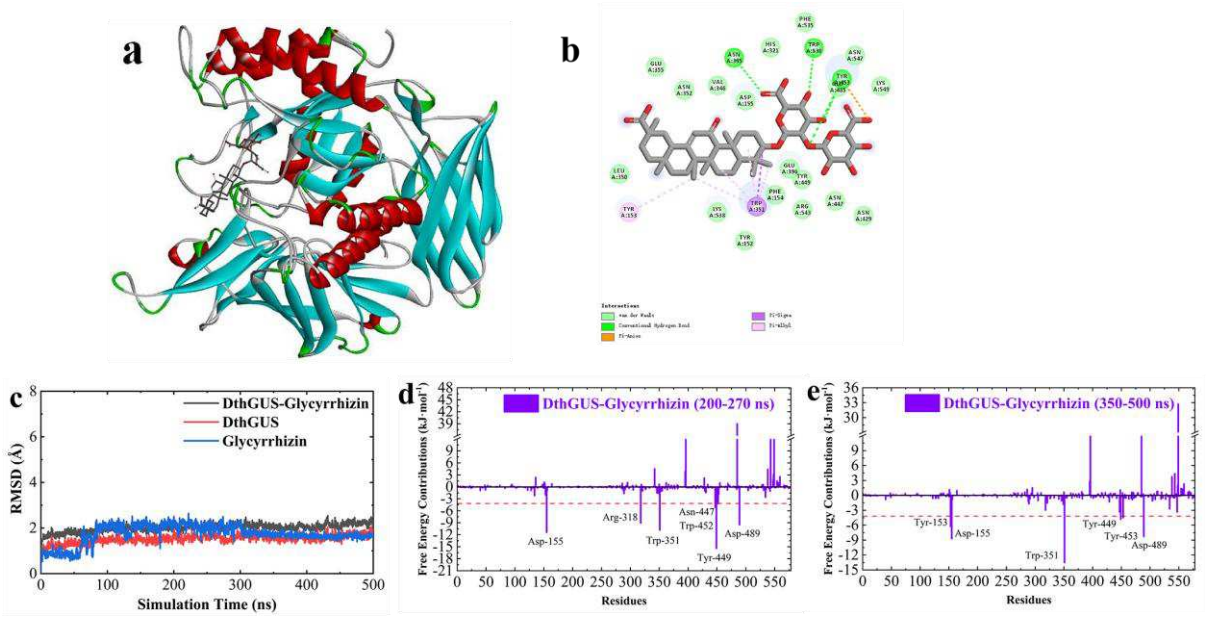


Fig. 10 DthGUS-glycyrrhizic acid binding and MD simulation **(a)** binding mode of DthGUS and glycyrrhizic acid; **(b)** structure of glycyrrhizic acid; **(c)** RMSD (root mean square deviation) curves of the DthGUS monomer, glycyrrhizic acid ligand, and DthGUS-glycyrrhizic acid complex during the 500 ns molecular dynamics simulation process; **(d-e)** contribution of each amino acid residue to the binding free energy of the DthGUS-pNPG complex in the simulation time periods of 200–270 ns and 350–500 ns, respectively. Red dotted lines mark the key residues with significant contributions

With the aim of exploring the molecular mechanism of β-glucuronidase DthGUS catalyzing the hydrolysis of glycyrrhizic acid, based on the previous molecular docking, a 500 ns MD simulation was also performed under the RSFF2C potential field to obtain the conformational movement details of GUS and glycyrrhizic acid during the binding process. The RMSD curves of the DthGUS-Glycyrrhizin complex and DthGUS displayed a slow increase at the beginning, reaching 2.1 Å and 1.6 Å respectively at 300 ns. These curves remained relatively stable in the subsequent MD simulation time. The RMSD curve of the ligand glycyrrhizic acid rose from 0.8 Å to 2.1 Å from 59 to 82 ns, then remained stable from 82 ns to 300 ns, and decreased to 1.7 Å at 300 ns, remaining stable in the 300-500 ns period.

Table 6 Binding free energy of DthGUS-glycyrrhizic acid complex(unit: kJ/mol)

System	Time scope (ns)	ΔG_{vdw}	ΔG_{ele}	ΔG_{PB}	ΔG_{SA}	ΔG_{bind}

	200-2	-229.595 ±	-181.306 ±	401.117 ±	-27.017 ±	-36.801 ±
DthGUS	70	24.781	27.608	26.682	1.841	31.426
-Glycyrrhizin	350-5	-250.133 ±	-122.761 ±	311.174 ±	-26.425 ±	-88.144 ±
	00	16.588	19.064	22.513	1.337	20.512

Table 7 Residue energy decomposition of the DthGUS-glycyrrhizic acid(unit: kJ/mol)

System	Time scope (ns)	Residues	ΔG_{MM}	ΔG_{PB}	ΔG_{SA}	ΔG_{bind}
DthGUS - Glycyrrhizin	200-270	Asp155	-7.435	-3.215	-0.761	-11.41
		Arg318	3.162	-12.264	0	-9.107
		Trp351	-14.558	5.217	-1.510	-10.839
		Asn447	1.453	-6.631	-0.006	-5.175
		Tyr449	-11.590	-2.765	-1.093	-15.438
		Trp452	-7.788	4.083	-0.513	-4.232
		Asp489	-0.725	-8.762	-0.038	-9.518
		Tyr153	-13.910	8.815	-1.178	-6.269
	350-500	Asp155	-9.723	1.716	-0.735	-8.736
		Trp351	-19.302	8.201	-2.422	-13.525
		Tyr449	-0.273	-4.497	-0.066	-4.833
		Tyr453	-6.765	3.313	-1.058	-4.519
		Asp489	-2.654	-5.627	0	-8.293

Table 6 lists the binding free energy (ΔG_{bind}) values of DthGUS and glycyrrhizic acid obtained based on the MD simulation trajectories at different time periods. As indicated by the table, the ΔG_{bind} value of the complex tends to increase from -36.801 ± 31.426 kJ/mol to -88.144 ± 20.512 kJ/mol. The van der Waals energy (ΔG_{vdw}), Coulombic electrostatic interaction energy (ΔG_{ele}), and non-polar solvation free energy (ΔG_{SA}) are dominant in the MD simulation process and significantly affect the binding affinity of the complex system. This interaction continuously drives the binding process of GUS and glycyrrhizic acid, ultimately manifested as GUS having the activity to catalyze the hydrolysis of glycyrrhizic acid molecules.

As indicated by the results of the free energy decomposition calculation in Table 7, the binding affinity of the key residues exceeding -4.18 kJ/mol was Asp155, Arg318, Trp351, Asn447, Tyr449, Trp452, and Asp489 in the 200-200ns simulation period of the DthGUS and glycyrrhizic acid complex system. Their ΔGbind values in the 150-200ns period reached -11.41 kJ/mol, -9.107 kJ/mol, -10.839 kJ/mol, -5.175 kJ/mol, -15.438 kJ/mol, -4.232 kJ/mol, and -9.518 kJ/mol, respectively. In the 350-500ns simulation period, the key residues with binding affinity exceeding -4.18 kJ/mol included Tyr153, Asp155, Trp351, Tyr449, Tyr453, and Asp489. Their ΔGbind values in the 350-500ns period were -6.269 kJ/mol, -8.736 kJ/mol, -13.525 kJ/mol, -4.833 kJ/mol, -4.519 kJ/mol, and -8.293 kJ/mol, respectively. The above-mentioned residues are of critical significance in the binding process of GUS and the glycyrrhizic acid complex, especially residue 155 and residue 351, which contribute to the binding catalysis of GUS and the glycyrrhizic acid complex in different time periods.

As depicted in Fig. 11, apart from the alkyl-π interaction formed between the side chains of GUS residues Asp155, Trp351 and Tyr153 and the benzene ring of the glycyrrhizic acid molecule, which significantly contributes to the binding ability of the GUS and glycyrrhizic acid complex system, the van der Waals energy and hydrogen bond interactions present in the complex system significantly affect the stability of the binding. Although the structure of glycyrrhizic acid undergoes a small movement within the DthGUS cavity in the MD dynamic equilibrium process, the stable alkyl-π interaction forces between Trp351 and other residues in DthGUS and the glycyrrhizic acid in the dominant conformation significantly contribute to the complex's stability. Thus, glycyrrhizic acid can stably bind in the GUS binding pocket, and it can be catalytically hydrolyzed by GUS into monoglucose glycyrrhizic acid and glycyrrhizic acid.

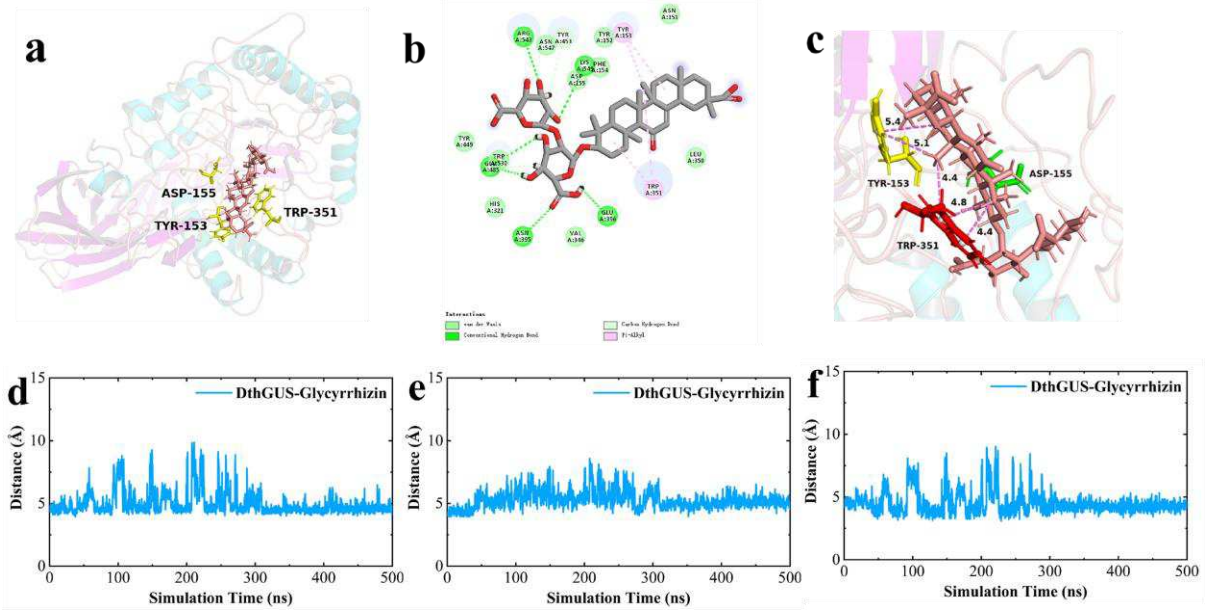


Fig. 11 Analysis of Key Interactions in the DthGUS-Glycyrrhizic Acid System for Molecular Dynamics Simulation. **(a)** key interactions of the DthGUS-glycyrrhizic acid system at equilibrium representing the conformational active site; **(b)** interaction pattern diagram of the conformation of the DthGUS-glycyrrhizic acid system from the MD simulation under the RSFF2C force field. The key residues of DthGUS and the molecular structure of glycyrrhizic acid are all represented by stick models; **(c)** distance visualization graph of the interactions between key residues and the glycyrrhizic acid molecule (unit: Å); **(d-f)** distance changes of the three π-alkyl interactions formed between the key residue Trp351 and the glycyrrhizic acid molecule over time

Discussion

This study successfully achieved heterologous recombinant expression and purification of β-glucuronidase from four thermophilic archaea, and systematically characterized the enzymatic properties of these recombinant enzymes, including the effects of pH, temperature, and metal ions on enzyme activity, as well as enzyme conversion efficiency. It was clarified that this archaeal glucuronidase possesses typical hyperthermophilic enzyme catalytic advantages and excellent environmental adaptability. The research results indicate that thermophilic archaeal β-glucuronidase shows significant advantages over most homologous enzymes from mesophilic microorganisms in high-temperature catalysis, structural stability, and tolerance to complex industrial environments. This provides high-quality archaeal enzyme resources and a theoretical basis for exploring extreme enzyme resources, biotransformation of glucuronide compounds, and applications of high-temperature industrial enzymes.

The research results show that *E. coli* Rosetta(DE3)/pET-28a-DthGUS has the highest enzyme activity. Its optimal pH is 5.0, and the optimal reaction temperature is 85 °C. This enzyme tends to lose activity upon prolonged exposure to strongly acidic conditions, while it exhibits good heat resistance. It has been reported that Mn^{2+} and Mg^{2+} exert no significant effect on DthGUS activity, whereas Zn^{2+}, Ga^{2+}, Cu^{2+}, Na^{+}, and K^{+} promote DthGUS activity. Among these ions, Fe^{2+} and Fe^{3+} produce a strong inhibitory effect on the enzyme, nearly abolishing its enzymatic activity. These results offer theoretical references for the subsequent application of this enzyme in glycyrrhizic acid hydrolysis to prepare monoglucuronic acid glycyrrhetic acid; namely, Fe^{3+} and other inhibitory metal ions should be prevented from contaminating and interfering with the hydrolysis conversion system, and low-temperature and weakly acidic environments favor the enzymatic reaction and storage of enzyme preparations.

As indicated by the experimental results of glycyrrhizic acid hydrolysis transformation, DthGUS exhibited excellent catalytic hydrolytic activity toward glycyrrhizic acid. DthGUS achieved a hydrolysis rate of 98.7% under the given conditions. It efficiently generated GAMG and glycyrrhetic acid in a targeted manner. GAMG can retain one glucuronic acid group and remove only one terminal glucuronic acid unit from the glycyrrhizic acid molecule. In general, chemical synthesis methods are subjected to poor selectivity, numerous by-products, and difficulties in separation and purification. Thus, it is challenging to efficiently produce this compound. In contrast, enzymatic hydrolysis, with its superior substrate regioselectivity, can specifically cleave the glycosidic bond in glycyrrhizic acid. On that basis, the efficient synthesis of GAMG can be achieved, and a strong support can be provided for the green bioproduction of GAMG.

Using *E. coli* Rosetta(DE3)/pET-28a-DthGUS, we performed an in-depth investigation into the hydrolysis mechanism by which GUS catalyzes pNPG and glycyrrhizic acid. First, based on the amino acid sequence of β-glucuronidase, we predicted the protein structural model and conducted molecular docking with pNPG and glycyrrhizic acid to obtain the optimal binding conformation of the complex systems. Subsequently, a 500 ns molecular dynamics simulation was performed under the RSFF2C force field. Results indicate that key residues Tyr153 and Trp351 play crucial roles in the binding and catalytic processes of DthGUS toward pNPG and glycyrrhizic acid. Alkyl-π interactions formed between the aromatic rings of side chains at this active site and those of pNPG and glycyrrhizic acid, together with strong hydrogen bonds and hydrophobic interactions, stabilize the complex systems and facilitate anchoring of pNPG and glycyrrhizic acid within the active cavity of DthGUS. The total binding free energy (ΔG_{bind}) values calculated via thermodynamic analysis for the two complex systems were -73.410 ± 12.935 kJ/mol and -88.144 ± 20.512 kJ/mol, respectively, indicating high binding affinities of DthGUS for both ligands and demonstrating its hydrolytic catalytic activity.

Currently, industrialized β-glucuronidase is mostly obtained from fermentation of mesophilic bacteria. Such enzymes have drawbacks including long fermentation cycles, low yields, poor stability and high production costs, which restrict the large-scale preparation of glycyrrhetic acid. Traditional chemical synthesis processes readily generate by-products, lowering product yield and purity, and produce substantial waste liquid that causes severe pollution. These issues bring heavy environmental burdens and high environmental costs. In contrast, thermophilic enzyme catalysis is green and efficient with fewer by-products; thermophilic enzymes feature high-temperature resistance and strong tolerance, rendering them better suited for large-scale industrial production and endowing them with broad application prospects. This study adopted thermophilic β-glucuronidase as the catalyst and glycyrrhetic acid as the substrate to prepare GAMG and glycyrrhetic acid. The

yields of both products from this process satisfy the basic industrialization requirements. In future work, catalytic process parameters will be further optimized, and the reaction system will be scaled up to advance the industrialization of this process. Moreover, through bioinformatics, the molecular modification of thermophilic enzymes will be performed to improve the enzyme yield and catalytic activity via directed evolution. Thus, technical support can be provided for the green and low-cost large-scale preparation.

Conclusion

The research results show that *E. coli* Rosetta (DE3)/pET-28a-DthGUS exhibits the highest enzyme activity at 123 U/μL. Its optimal reaction conditions are pH 5.0 and 85 °C. The enzyme tends to undergo inactivation under conditions of pH < 4.5. K^+, Zn^{2+}, Cu^{2+}, and Ca^{2+} can activate enzyme activity, whereas Fe^{2+} and Fe^{3+} will cause the enzyme to lose activity. After an 8 h reaction under optimal conditions, the hydrolysis rate of glycyrrhizic acid reaches 98.7%. Molecular dynamics simulation results indicate that Tyr153 and Trp351 serve as key residues for catalysis of pNPG and glycyrrhizic acid, respectively. The binding free energies of DthGUS with pNPG and glycyrrhizic acid respectively reach -73.410 ± 12.935 kJ/mol and -88.144 ± 20.512 kJ/mol. As revealed by the above findings, this enzyme has good binding and catalytic hydrolysis capabilities for both substrates.

Acknowledgements

Not applicable.

Author contributions

D.X. proposed the idea. D.X., M.L., Q,G., M.R., X,W., and Y.X. designed the research protocol. D.X., M.L., M.R., Y,Y., and X,W. conducted the experimental preparation and data analysis.The initial draft of the article was co-prepared by D.X., M.L., and M.R., and edited and reviewed by M.L., M.R., C.W., D.X., and F,L. All authors have read and approved the published version of the manuscript.

Funding

This work was financially supported by the University Synergy Innovation Program of Anhui Province (Grant No. GXXT-2023-107), the Anhui Province University Outstanding Talents Cultivation Funding Project (Grant No. gxgnfx2021118), and the Anhui Province Quality Project (Biological Engineering Services for the Emerging Industries of Anhui Province, Grant No. 2025fwxx029).

Data availability

Date will be made available on request.

Declarations

Ethical approval

Not applicable.

Consent to participate

Not applicable.

Consent for publication

All authors agree to publishing this manuscript with Microbial Cell Factories.

Competing interests

The authors declare no competing interests.

References

1. Henrissat B, Davies G. Structural and sequence-based classification of glycoside hydrolases. *Curr. Opin. Struct. Biol.* 1997;7:637–44. https://doi.org/10.1016/s0959-440x(97)80072-3.
2. Paigen K. Mammalian beta-glucuronidase: genetics, molecular biology, and cell biology. *Prog. Nucleic Acid Res. Mol. Biol.* 1989;37:155–205. https://doi.org/10.1016/s0079-6603(08)60698-4.
3. Xiao Y, Zhang Z, Liang W, Gao B, Wang Y, Chang J, Zhu D. Endophytic fungi from Dongxiang wild rice (Oryza rufipogon Griff.) show diverse catalytic potential for converting glycyrrhizin. *3 Biotech.* 2022;12:79. https://doi.org/10.1007/s13205-022-03138-x.
4. Xu Y, Feng X, Jia J, Chen X, Jiang T, Rasool A, Lv B, Qu L, Li C. A Novel β-Glucuronidase from Talaromyces pinophilus Li-93 Precisely Hydrolyzes Glycyrrhizin into Glycyrrhetinic Acid 3-O-Mono-β-d-Glucuronide. *Appl. Environ. Microbiol.* 2018;84:e00755-18. https://doi.org/10.1128/AEM.00755-18.
5. Kim DH, Lee SW, Han MJ. Biotransformation of glycyrrhizin to 18beta-glycyrrhetinic acid-3-O-beta-D-glucuronide by Streptococcus LJ-22, a human intestinal bacterium. *Biol. Pharm. Bull.* 1999;22:320–2. https://doi.org/10.1248/bpb.22.320.
6. Akao T, Akao T, Kobashi K. Glycyrrhizin stimulates growth of Eubacterium sp. strain GLH, a human intestinal anaerobe. *Appl. Environ. Microbiol.* 1988;54:2027–30. https://doi.org/10.1128/aem.54.8.2027-2030.1988.
7. Wu Q, Guo Q, Yang F, Li M, Zhu Y, Xu B, Zhao L, Zhang S, Xie Y, Li F, Wu X, Xu D. Heterologous Expression and Enzymatic Properties of β-Glucuronidase from Clostridium perfringens and Its Application in Bilirubin Transformation. *Microorganisms.* 2025;13:1043. https://doi.org/10.3390/microorganisms13051043.
8. Henrissat B, Davies GJ. Glycoside hydrolases and glycosyltransferases. Families, modules, and implications for genomics. *Plant Physiol.* 2000;124:1515–9. https://doi.org/10.1104/pp.124.4.1515.
9. Jefferson RA, Kavanagh TA, Bevan MW. GUS fusions: beta-glucuronidase as a sensitive and versatile gene fusion marker in higher plants. *EMBO J.* 1987;6:3901–7. https://doi.org/10.1002/j.1460-2075.1987.tb02730.x.
10. Bramwell KK, Ma Y, Weis JH, Chen X, Zachary JF, Teuscher C, Weis JJ. Lysosomal β-glucuronidase regulates Lyme and rheumatoid arthritis severity. *J. Clin. Invest.* 2014;124:311–20. https://doi.org/10.1172/JCI72339.

11. Sakurama H, Kishino S, Uchibori Y, Yonejima Y, Ashida H, Kita K, Takahashi S, Ogawa J. β-Glucuronidase from Lactobacillus brevis useful for baicalin hydrolysis belongs to glycoside hydrolase family 30. *Appl. Microbiol. Biotechnol.* 2014;98:4021–32. https://doi.org/10.1007/s00253-013-5325-8.
12. Li JY, Cao HY, Liu P, Cheng GH, Sun MY. Glycyrrhizic acid in the treatment of liver diseases: literature review. *Biomed. Res. Int.* 2014;2014:872139. https://doi.org/10.1155/2014/872139.
13. Chen RY, Shi JJ, Liu YJ, Yu J, Li CY, Tao F, Cao JF, Yang GJ, Chen J. The State-of-the-Art Antibacterial Activities of Glycyrrhizin: A Comprehensive Review. *Microorganisms.* 2024;12:1155. https://doi.org/10.3390/microorganisms12061155.
14. Hoever G, Baltina L, Michaelis M, Kondratenko R, Baltina L, Tolstikov GA, Doerr HW, Cinatl J Jr. Antiviral activity of glycyrrhizic acid derivatives against SARS-coronavirus. *J. Med. Chem.* 2005;48:1256–9. https://doi.org/10.1021/jm0493008.
15. Han S, Sun L, He F, Che H. Anti-allergic activity of glycyrrhizic acid on IgE-mediated allergic reaction by regulation of allergy-related immune cells. *Sci. Rep.* 2017;7:7222. https://doi.org/10.1038/s41598-017-07833-1.
16. Robe PA, Princen F, Martin D, Malgrange B, Stevenaert A, Moonen G, Gielen J, Merville M, Bours V. Pharmacological modulation of the bystander effect in the herpes simplex virus thymidine kinase/ganciclovir gene therapy system: effects of dibutyryl adenosine 3',5'-cyclic monophosphate, alpha-glycyrrhetinic acid, and cytosine arabinoside. *Biochem. Pharmacol.* 2000;60:241–9. https://doi.org/10.1016/s0006-2952(00)00315-4.
17. Cao M, Zuo J, Yang JG, Wu C, Yang Y, Tang W, Zhu L. Physiology-Based Pharmacokinetic Study on 18β-Glycyrrhetic Acid Mono-Glucuronide (GAMG) Prior to Glycyrrhizin in Rats. *Molecules.* 2022;27:4657. https://doi.org/10.3390/molecules27144657.
18. Baltina LA. Chemical modification of glycyrrhizic acid as a route to new bioactive compounds for medicine. *Curr. Med. Chem.* 2003;10:155–71. https://doi.org/10.2174/0929867033368538.
19. Wu SY, Wang WJ, Dou JH, Gong LK. Research progress on the protective effects of licorice-derived 18β-glycyrrhetinic acid against liver injury. *Acta Pharmacol. Sin.* 2021;42:18–26. https://doi.org/10.1038/s41401-020-0383-9.
20. Kowalska A, Kalinowska-Lis U. 18β-Glycyrrhetinic acid: its core biological properties and dermatological applications. *Int. J. Cosmet. Sci.* 2019;41:325–331. https://doi.org/10.1111/ics.12548.
21. Park M, Lee JH, Choi JK, Hong YD, Bae IH, Lim KM, Park YH, Ha H. 18β-glycyrrhetinic acid attenuates

anandamide-induced adiposity and high-fat diet induced obesity. *Mol. Nutr. Food Res.* 2014;58:1436–46. https://doi.org/10.1002/mnfr.201300763.

22. Yoqubova N, Gulyamov S, Abdulla-Zoda D, Tursunov K, Sharipov A, Rizaev K, Hu X. Glycyrrhetinic Acid in Cancer Therapy: Mechanistic Insights, Therapeutic Potential, and Future Directions. *Anticancer Agents Med. Chem.* 2026. https://doi.org/10.2174/0118715206440313260127193145.
23. Park NY, Kim C, Park HS, Kim SG, Lee J. Glycyrrhetinic Acid and Autocrine Motility Factor Converge on G6PD Suppression, Oxidative Stress, and Drug Retention to Impair Pancreatic Ductal Adenocarcinoma Cell Growth. *Anticancer Res.* 2026;46:4301–4309. https://doi.org/10.21873/anticanres.18288.
24. Wang Y, Xue P, Cao M, Yu T, Lane ST, Zhao H. Directed Evolution: Methodologies and Applications. *Chem. Rev.* 2021;121:12384–12444. https://doi.org/10.1021/acs.chemrev.1c00260.
25. Ding Y, Perez-Ortiz G, Peate J, Barry SM. Redesigning Enzymes for Biocatalysis: Exploiting Structural Understanding for Improved Selectivity. *Front. Mol. Biosci.* 2022;9:908285. https://doi.org/10.3389/fmolb.2022.908285.
26. Vornholt T, Stockinger P, Mutný M, Jeschek M, Nestl B, Oberdorfer G, Osuna S, Pleiss J, Welner DH, Krause A, Buller R, Ward TR. Of Revolutions and Roadblocks: The Emerging Role of Machine Learning in Biocatalysis. *ACS Cent. Sci.* 2025;11:1828–1838. https://doi.org/10.1021/acscentsci.5c00949.
27. Waterhouse AM, Procter JB, Martin DM, Clamp M, Barton GJ. Jalview Version 2--a multiple sequence alignment editor and analysis workbench. *Bioinformatics.* 2009;25:1189–91. https://doi.org/10.1093/bioinformatics/btp033.
28. Li Q, Jiang T, Liu R, Feng X, Li C. Tuning the pH profile of β-glucuronidase by rational site-directed mutagenesis for efficient transformation of glycyrrhizin. *Appl. Microbiol. Biotechnol.* 2019;103:4813–4823. https://doi.org/10.1007/s00253-019-09790-3.
29. Zhang Y, Skolnick J. The protein structure prediction problem could be solved using the current PDB library. *Proc. Natl. Acad. Sci. U. S. A.* 2005;102:1029–34. https://doi.org/10.1073/pnas.0407152101.
30. Liu Y, Huangfu J, Qi F, Kaleem I, E W, Li C. Effects of a non-conservative sequence on the properties of β-glucuronidase from Aspergillus terreus Li-20. *PLoS One.* 2012;7:e30998. https://doi.org/10.1371/journal.pone.0030998.
31. Dill KA, Ozkan SB, Shell MS, Weikl TR. The protein folding problem. *Annu. Rev. Biophys.* 2008;37:289–316. https://doi.org/10.1146/annurev.biophys.37.092707.153558.